PART II

PART II Result of the Third Year's Investigation

Chapter 1 Geophysical Prospecting

Geophysical surveys using a gravity and IP methods are carried out around four mineral indications in the Oued Jebes prospect located in the northeast part of the project area. The additional geophysical surveys in the El Akhouat prospect are followed up the result of the first phase and the second. The methodology and the results of the geophysical surveys are described below.

1.1 Outline of Survey

1.1.1 Survey Prospect

The Oued Jebes prospect applied geophysical prospecting is shown on the figure 5 as the geophysical survey area map.

The Oued Jebes prospect is located in the west-southwest of approximately 60km from Tunis, which is the capital of Tunisia. It takes about one hour to the prospect from Tunis by car on the national road towards Beja, which is the city in the northwest Tunisia.

Five mineral indications are known in this prospect. Four survey sub-prospects of approximately 1 km wide and from 2 to 2.5 km long were laid around those mineral indications. These sub-prospects are called OA, OB, OC and OD area.

The El Akhouat prospect applied the additional geophysical prospecting is shown on the figure 6 as the geophysical survey area map.

The four sub-prospects in the Oued Jebes prospect are presented below. The El Akhouat prospect has already been described in the report of the first phase.

(1) OA sub-prospect

This sub prospect lies at the around 3km south of Mejez el Bab in the northeast end of the Krib – Mejez Elbab area. The base line was laid out along the axis of the Djebel Bou Mouss hills extending in the NE-SW direction. The sub-prospect is a rectangular area of 1km wide in the NW-SE direction and almost centered the base line. National coniferous forests cover the northwest part ranging a couple of hundreds metre from the base line. Fields of wheats and legumes dominate the other part of the sub-prospect. The Djebel Bou Mouss hills consist of cretaceous limestones. A triassic diapir appears in the northwest side slope of the hills. The plain over tertiary sedimentary rocks is extended in the southeast side of them.

There is old workings of the Bou Mouss mineral indication at the boundary between triassic system and cretaceous in the southwest part of the sub-prospect.

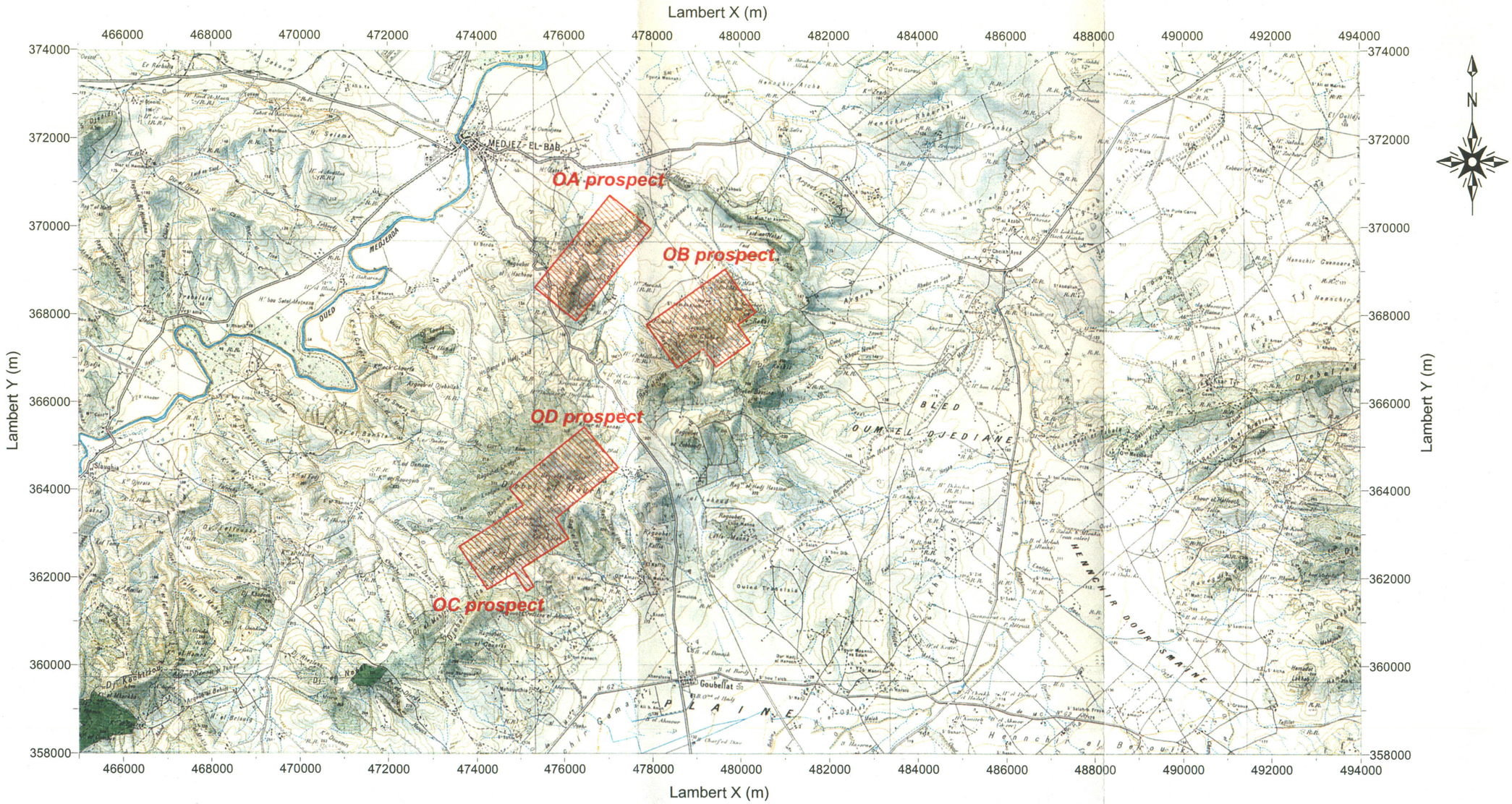

Figure 5 Geophysical survey area map

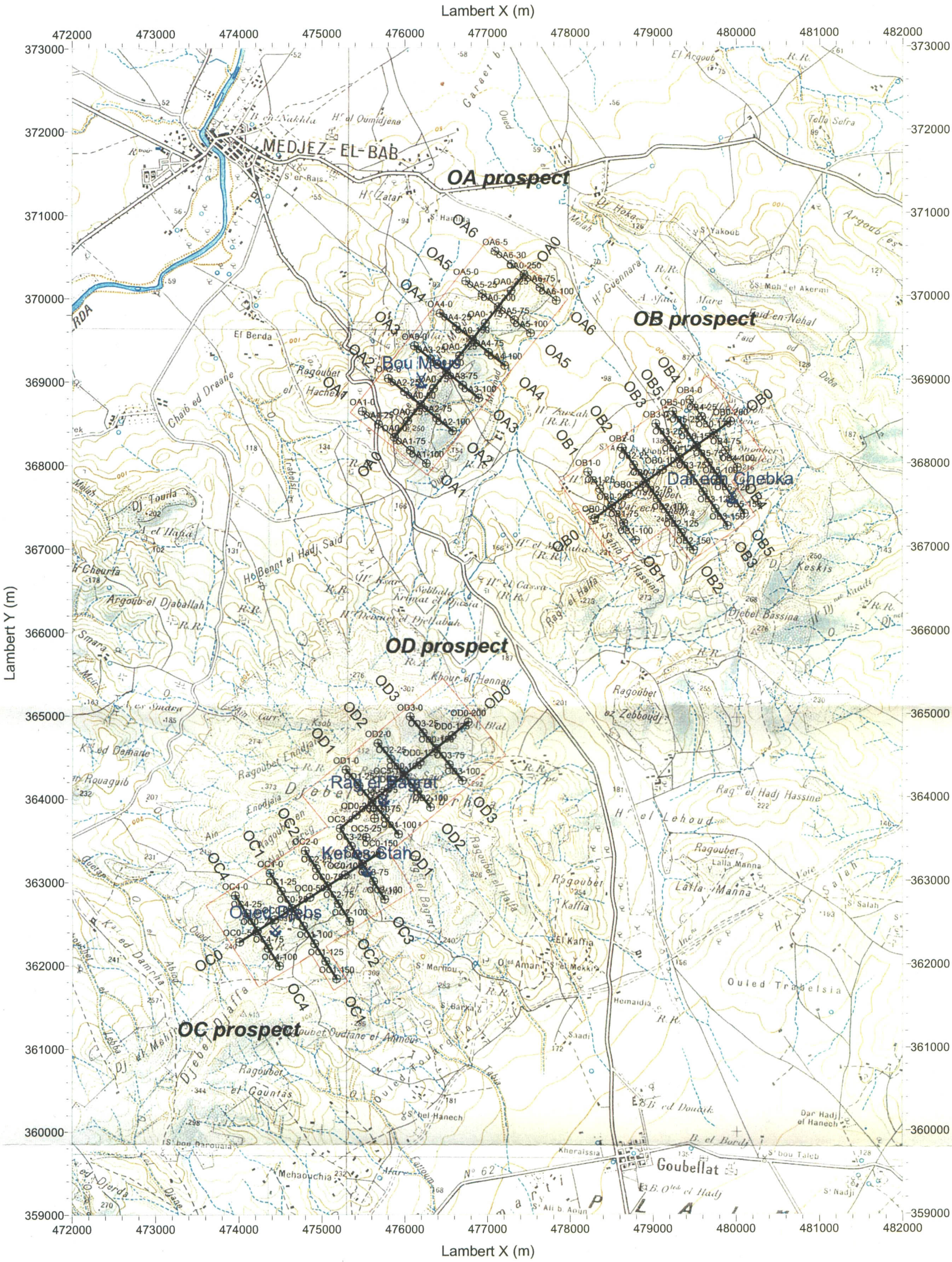

Figure 6 Layout of geophysical survey line in Oued Jebs prospect

(2) OB sub-prospect

This sub-prospect is located in the approximately 2 km northeast of the OA sub-prospect. It lies in the northwest side slopes of hills from Dar ech Chebka to Bou Rahal. The base line of 2 km long runs parallel to the axis of the hills at the northwest foothill, and the sub-prospect is centered 1 km wide by the base line. The slope area is covered with grassy and shrubbery vegetation, and wheat fields extend in the hilltop and foothill areas.

A triassic diapir appears at the slope area in the central part of the sub-prospect. The triassic system is contacted with cretaceous system in the northwest side, tertiary system in the southeast side. A small old working of the Dar ech Chebka mineral indication is left in the tertiary system area.

(3) OC and OD sub-prospects

These sub-prospects lies from the central part to southeast part of the Djebel el Mouhra hills located around 4 km in the opposite side of the road connecting between Mejez el Bab and Goubellat to the OB prospect. They are bordered around the Kef Lasfer mineral indication. The OC sub-prospects of 1 km wide is centered the base line of 2 km long along the Oued Jebes stream in the west part of the hills. The boundary of the OD sub-prospect is a rectangular of 2 km long and 1 km wide in the northeast part of them. Both sub-prospect are dominant with national coniferous forests, except for the partly wheat and olive fields.

The northwest side from the center of the hills consists of triassic diapers, geology in the other southeast side changes from cretaceous system to tertiary system.

Relatively large old working of the Oued Jebes mineral indications neighboring the Oued Jebes stream in the west part of the hills is known. The Kef Lasfer mineral indication with small old galleries is located on the boundary between the OC and the OD sub-prospect. There are also small old galleries of the Rag el Bagrat mineral indication in the northeast of an approximately 600 m from the Kef Lasfer.

1.1.2 Applied Technique and Amount

Geophysical surveys using a gravity and IP methods are applied for the both prospects. Their survey amount is shown in the following Table 4.

Table 4 Amount of Geophysical Survey

Method	Item	Oued Jebes prospect				El Akhouat – Argoub Adama prospect	Total
		OA	OB	OC	OD		
Gravity	Station	35	35	27	20	6	123
IP	Length	5.5km	6.5km	5.5km	5km	3.5km	26km
	Measurment	195	245	195	170	115	920

In ordert to carry out geophysical surveys, a baseline is set through each prospect and traverses are laid out perpendicularly to baselines. Their identifications of stations, length, position and so on are shown from the Table 5 to 6.

Table 5 Specification of geophysical survey lines in Oued Jebes prospect

Line	Stations	Length (km)	Angle	Crossing to baseline	x(UTM)	y (UTM)	Applied Survey
OA0	51 (0~250)	2.5	N38°E		556359.97	4052133.83	Gravity IP
					557912.53	4054093.16	
OA1	21 (0~100)	1	N52°W	OA0-0	555968.14	4052444.34	Gravity
					556751.84	4051823.31	
OA2	21 (0~100)	1	N52°W	OA0-50	556278.65	4052836.21	Gravity IP
					557062.35	4052215.18	
OA3	21 (0~100)	1	N52°W	OA0-100	556589.16	4053228.07	Gravity IP
					557372.86	4052607.05	
OA4	21 (0~100)	1	N52°W	OA0-150	556899.67	4053619.94	Gravity IP
					557683.37	4052998.91	
OA5	21 (0~100)	1	N52°W	OA0-200	557210.18	4054011.81	Gravity
					557993.89	4053390.78	
OA6	21 (0~100)	1	N52°W	OA0-250	557520.69	4054403.67	Gravity
					558304.40	4053782.65	
OB0	41 (0~200)	2	N34°E		558793.86	4051181.53	Gravity IP
					560415.49	4052352.01	
OB1	21 (0~100)	1	N56°W	OB0-25	558703.96	4051733.26	Gravity
					559289.18	4050922.43	
OB2	31 (0~150)	1.5	N56°W	OB0-75	559109.36	4052025.87	Gravity IP
					559987.20	4050809.64	
OB3	31 (0~150)	1.5	N56°W	OB0-125	559514.77	4052318.50	Gravity IP
					560392.61	4051102.26	
OB4	21 (0~100)	1	N56°W	OB0-175	559920.17	4052611.11	Gravity
					560505.40	4051800.29	
OB5	31 (0~150)	1.5	N56°W	OB0-150	559717.47	4052464.80	Gravity IP
					560595.31	4051248.57	
OC0	41 (0~200)	1	N36°E		554549.21	4046075.95	Gravity IP
					556231.38	4047157.61	
OC1	21 (0~100)	1	N54°W	OC0-75	554909.61	4046902.11	Gravity IP
					555720.84	4045640.48	
OC2	21 (0~100)	1	N54°W	OC0-125	555330.15	4047172.43	Gravity IP
					555870.97	4046331.45	
OC3	21 (0~100)	1	N54°W	OC0-175	555750.69	4047442.94	Gravity IP
					556291.52	4046601.86	
OC4	21 (0~100)	1	N54°W	OC0-25	554489.07	4046631.79	Gravity IP
					555029.89	4045790.60	
OD0	41 (0~200)	1	N38°E		555750.69	4047442.94	Gravity IP
					557281.67	4048729.73	
OD1	21 (0~100)	1	N52°W	OD0-50	555811.73	4048147.40	Gravity IP
					556455.15	4047381.89	
OD0	21 (0~100)	1	N52°W	OD0-100	556194.47	4048469.10	Gravity IP
					556837.89	4047703.58	
OD1	21 (0~100)	1	N52°W	OD0-150	556577.22	4048790.79	Gravity IP
					557220.63	4048025.27	

Table 6 Specification of geophysical survey lines in El Akhouat prospect

Line	Stations	Length (km)	Angle	Crossing to Base Line	x(UTM)	y (UTM)	Applied Survey
L4	21 (0~100)	1	N62°W	L0-75	520591.26	4014709.64	IP
					521478.18	4014247.78	
L6	31 (0~150)	1.5	N62°W	L0-125	520378.74	4015384.02	Gravity IP
					521709.11	4014691.22	
L9	21 (0~100)	1	N62°W	L0-200	521168.59	4015818.27	Gravity IP
					522055.51	4015356.41	

Density, resistivity and chargeability as base data for interpreting results of the geophysical surveys are measured in laboratory for 21 samples collected from outcrops within and around the Oued Jebes prospects.

1.2 Methodology

1.2.1 Layout of Measuring Lines

The 22 survey lines within the Oued Jebes propect and the 3 lines within the El Akhouat propect are laid out by open traverse surveying using an electro-optical distance meter and a transit compass. Measuring stations are set along each line principally at an interval of 50 m and marked by wooden pickets. Each measuring station identifies itself by the number of relevant line and one tenth of the distance from the initial station of the line, that is, the measuring station OC0-125 indicates its position at 1250 m from the initial station of the line OC0.

Within the OA sub-prospect in the Oued Jebes prospect, the baseline OA0 with a total length of 2,500 m is set along the axis of the Djebel Bou Mous hills. Other 6 survey lines, 1,000 m long each, are laid out perpendicularly to the baseline at an interval of 500 m with the initial stations at their northwestern ends.

Within the OB sub-prospect, the baseline OB0 with a total length of 2,000 m is set along the northwest side boundary of the triassic diapir with cretaceous system. Four survey lines with 1,000 m long each, the line number from OB1 through OB4, are laid out perpendicularly to the baseline at an interval of 500 m with the initial stations at their northwestern ends. The survey line OB5 runs through the Dar ech Chebka mineral indication in the middle between the line OB3 and the OB4. The survey line OB2, OB3 and OB5 are extended 500 m towards the southeast in order to reach the mineral indication zone.

Within the OC sub-prospect, the baseline OC0 with a total length of 2,000 m is set connecting two mineral indications of the Oued Jebes and the Kef Lasfer. Four survey lines with 1,000 m long each, the line number from OC1 through OC4, are laid out perpendicularly to the baseline at an interval of 500 m with the initial stations at their northwestern ends. The survey line OC1 is extended 500 m towards the southeast

because a chargeability anomaly was found around the measurement point OC1-100.

Within the OD sub-prospect, the baseline OD0 with a total length of 2,000 m is set through the Rag el Bagrat mineral indication. Other three survey lines with 1,000 m long each, the line number from OD1 through OD3, are laid out perpendicularly to the baseline at an interval of 500 m with the initial stations at their northwestern ends.

Within the El Akhouat – Argoub Adama prospect, three survey lines, the line L4, L6 and L9, are laid out perpendicularly to the baseline set in the first phase of this project.

The coordinates of these survey lines are correlated by surveying to the benchmarks which have been located by the National Office of Topography. Since the coordinate system used for the surveying is the northern Tunisia surveying coordination by the Lambert Projection (hereinafter called Lambert Coordinate System), all coordinates are transformed to the UTM (Universal Transverse Mercator Projection) and the Geographical Coordinate Systems with the courtesy of ONM. of all outputs of the current investigation, the geophysical maps are prepared in accordance with the Lambert Coordinate System, on which all existing topographic, geologic, regional Bouguer anomaly maps are based. The elevation of each measuring station is determined by leveling using a digital auto-level, Model SDL30-1, manufactured by Sokia Co., Ltd., in order to achieve the accuracy of 10 cm $\pm$ required for the gravity survey.

1.2.2 Gravity Survey

Acceleration of gravity at the total of 123 stations on the 22 survey lines in the Oued Jebes prospect and the 2 lines in the El Akhouat – Argoub Adama prospect is measured. Principal interval among measured stations is 250 m.

The flow chart of the current gravity survey is shown in Figure 7.

In the neighboring area, the gravity survey project, CG-04, was carried out with a density of one measuring point for an approximately one square kilometer by ONM in 2000. Its survey data within the Mejez el Bab quadrangle is offered from ONM. The Bouguer anomaly map of the Mejez el Bab quadrangle shown Figure 8 is created using the data.

Relative gravity to that at the known station is measured using a gravimeter, Model G with a detection accuracy of 0.1 μgal, manufactured by La Coste & Romberg Co., Ltd. The gravity base station ST1000 of the current survey is set at the courtyard of the Emir hotel in Gâafour located in the south of the current prospects. ST1000's gravity value is decided by using relative measurement between the bases of the ONM gravity program CG-02 ant it. Gravity is measured once or more every day at the gravity base station for each closing gravity traverse. The maximum error for one closing gravity traverse is recorded at 0.1 mgal throughout the current survey.

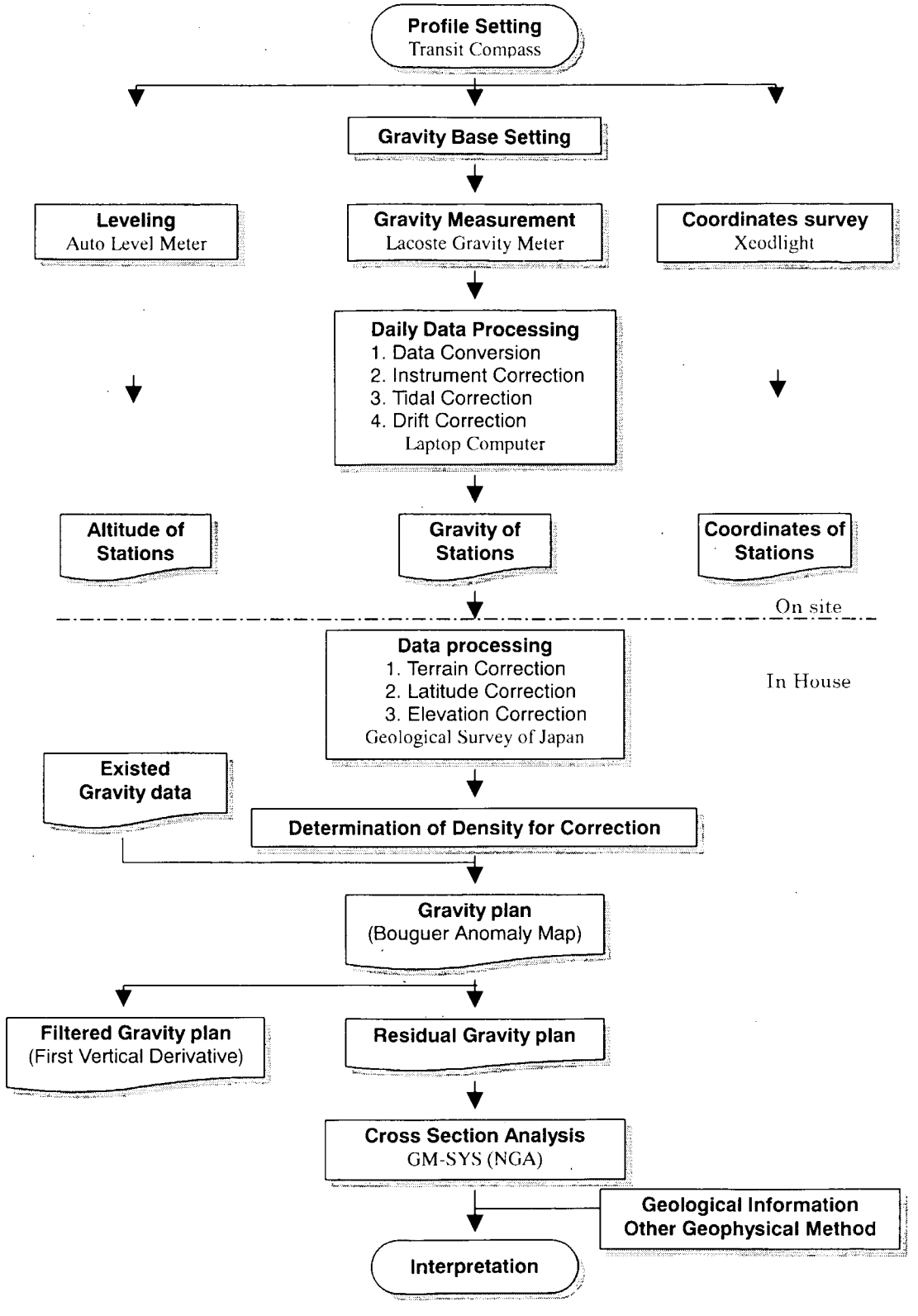

Figure 7 Flow Chart of Gravity Survey

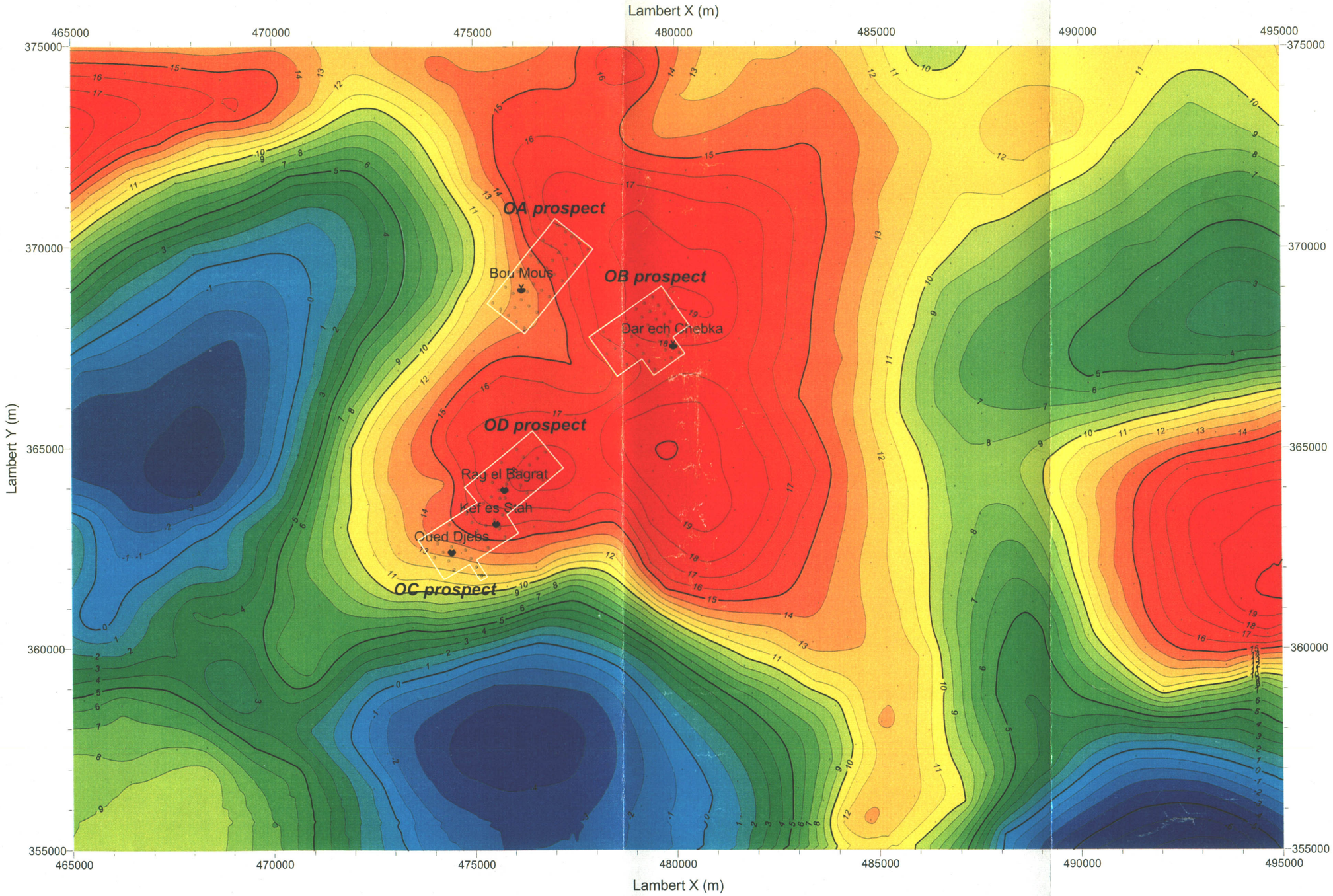

Figure 8 Reagional gravity map (Density : 2.4g/cm^3)

A gravity value, *ABSG* (mgal), at each measuring station is estimated using a relative gravity, *RG*, at the measuring point and the gravity value, *ABSG*, at the gravity base station as follows;

$$ABSG(\text{measuring point}) = RG(\text{measuring station}) - RG(\text{base}) + ABSG(\text{base}) \quad (1)$$

where,

$$RG = reading * factor + C_{inst} + C_{tidal} + C_{drift} \quad (2)$$

reading: instrumental reading, *factor*: reading－coefficient of conversion

C_{inst}: correction for instrument height, C_{tidal}: tidal correction

C_{drift}: drift correction.

A Bouguer gravity value, *Ab* (mgal), is also estimated for each measured gravity value (*ABSG*) using the following equation;

$$Ab = ABSG - G_{stand}(\phi) + C_{atm}(h) + C_{free}(h) + Cb(h, \gamma) + T(h, \gamma) \quad (3)$$

ϕ: latitude of measuring point, h: elevation of measuring point(m)

γ: specific gravity of rocks in the vicinity of measuring point(g/cm^3)

where

- Standard Gravity Value (1967 formula)

$$G_{stand}(\phi) = 978031.85(1+0.005278895 \sin^2 \phi + 0.000023462 \sin^4 \phi) \quad (4)$$

- Atmospheric Correction

$$C_{atm}(h) = 0.87 - 0.000965 h \quad (5)$$

- Free-air Correction

$$C_{free}(h) = (\partial g / \partial h) h = 0.3086 \text{ h} \quad (6)$$

- Bouguer Correction

$$Cb(h, \gamma) = -2 \pi G \gamma h = -0.04192 \gamma h \quad (7)$$

π: circular constant, G: universal gravitation constant

- Topographic Correction: T(h, γ)

  adopting the Topographic Correction Formula of GSJ (Geological Survey of Japan), established in 1989 by its Gravity Survey Research Group.

The density in the vicinity of measuring stations, which is used for the Bouguer and topographic corrections, is usually determined by an appropriate judgments taking account of densities estimated according to the following means;

① the result of density measurement of rock samples.

② the gradient of G-H correlation diagram.

G-H correlation diagram (Figure 12): produced by plotting measurements on a diagram with the abscissa for the differences between measured and standard gravity values against the ordinate for the elevation differences between measuring points.

③ comparison of the topographic map with Bouguer anomaly maps for several assumed densities: selecting the density least correlated to the topography.

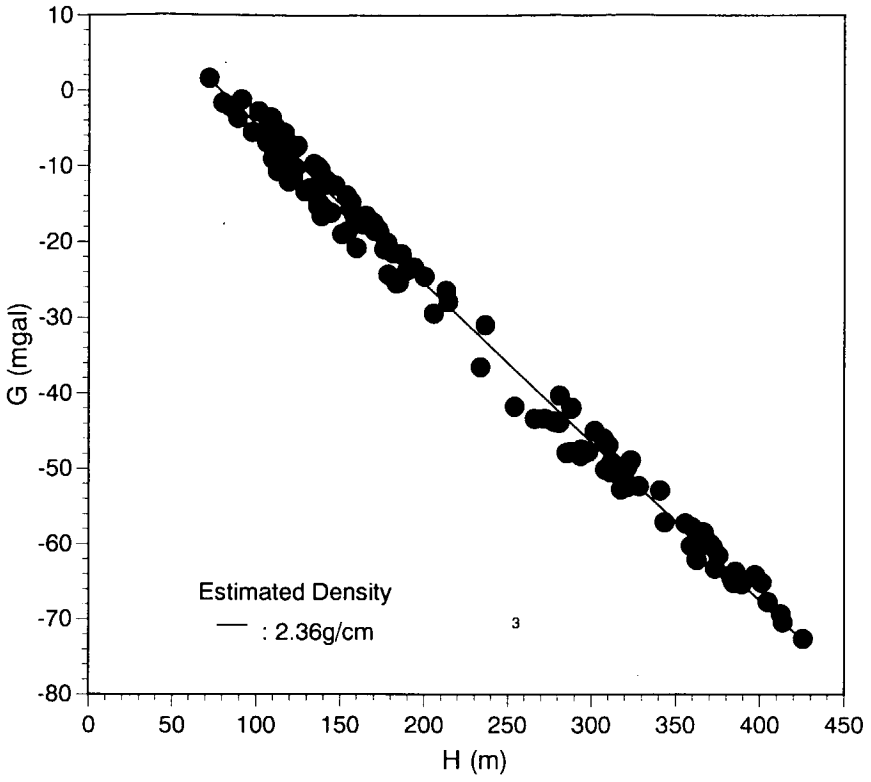

Figure 9 G-H correlation diagram for the Oued Jebes prospect

The average of density measurement of rock samples collected in and near the current prospects is 2.53 g/cm^3. A density of 2.36 g/cm^3 is obtained on the basis of the G-H diagrams for the Oued Jebes prospect. Besides, the Bouguer anomaly maps for the densities of 2.3 and 2.4 are judged to be relatively low in their correlativity with the topographic map. Taking these results into consideration, the correction densities of 2.4 g/cm^3 for the Oued Jebes prospect is adopted in the current gravity survey for the purpose of comparison.

Horizontal distribution of Bouguer gravity values comprises composite of shorter and longer spatial wavelength variations of gravity in the region as illustrated in Figure 10. The shorter wavelength variation reflects density variation of rocks in the shallower part of earth and the longer wavelength variation, that in the deeper part, several kilometers or deeper from the surface. The Bouguer gravity values of the current prospects, after estimation of 2-dimensional Fourier transform, are plotted on the power spectrum diagram (Figure 11) with the abscissa for wave number (spatial frequency) against the ordinate for natural logarithm of spectrum power. According to the diagram, the Bouguer gravity anomaly of the Oued Jebes prospect is composed of three components with their average depths at 1,105 m, 98 m and 37 m. Since the current gravity survey is concerned with prospecting ore deposits shallower than a few kilometers, it is tried to extract a shorter wavelength, that is, shallow component from

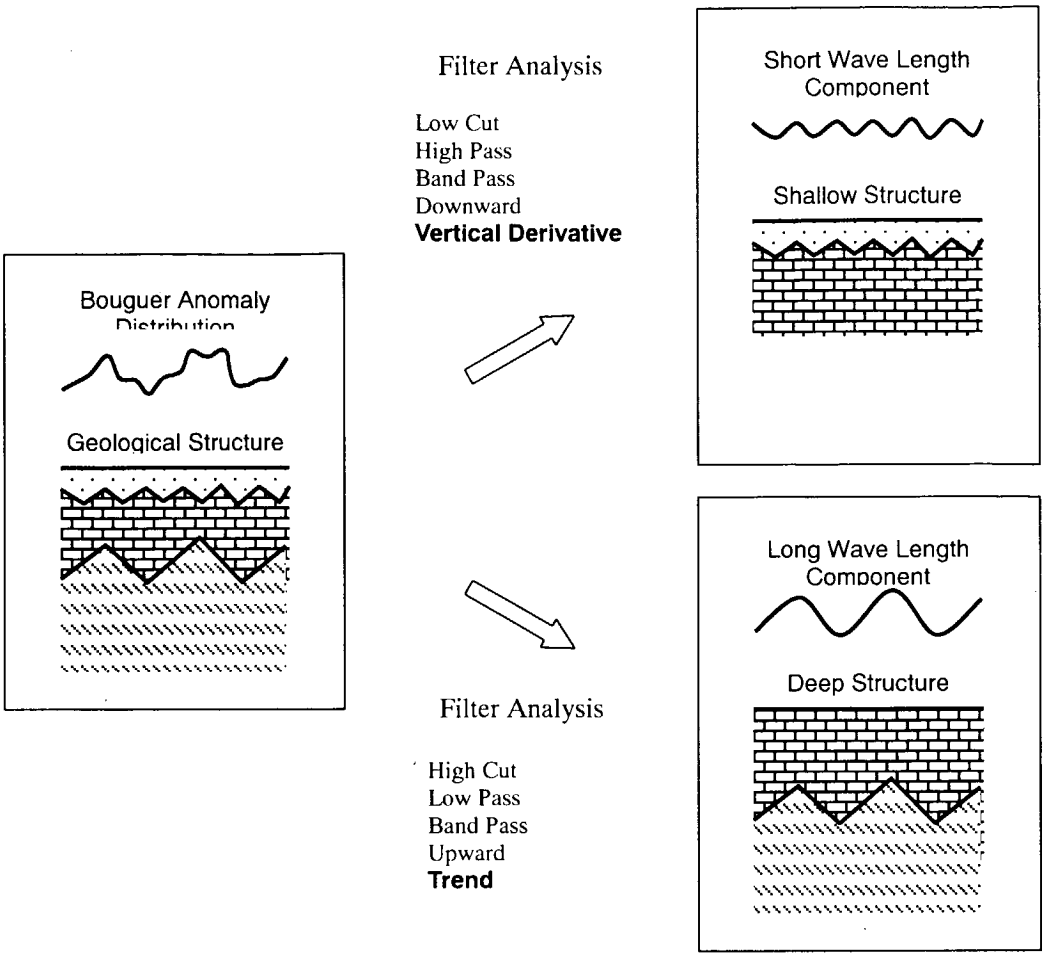

Figure 10 Schematic Diagram of Filter Analysis in Gravity Survey

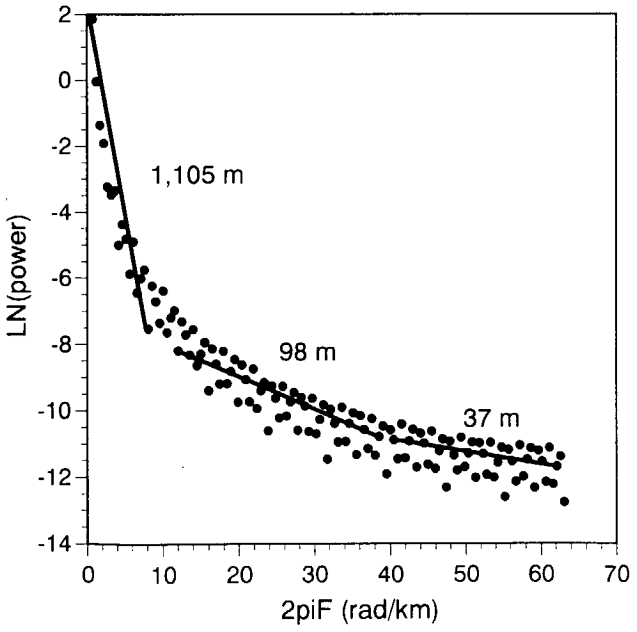

Figure 11 Power Spectrum Diagram for the Oued Jebes prospect

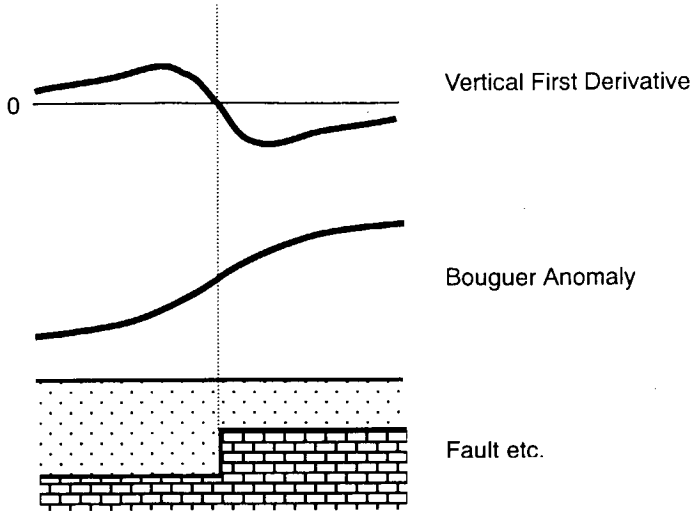

Figure 12 Enhancement of Vertical First Derivative Filter

the Bouguer anomaly map.

For extracting the shorter wavelength component, one approach is to use a low-cut or band-pass filter for data processing and the other, to estimate residuals over a regional trend surface of Bouguer gravity values. In the current survey, the first vertical derivative filter, a kind of low-cut filter, and the trend surface analysis are adopted for extracting the shorter wavelength component.

The result of first vertical derivative filtering is shown in the first vertical derivative anomaly map. The 0 contour between the positive maximum and the negative minimum indicates a boundary between two subsurface geologic bodies with different density structures, e.g. a fault, a intrusive contact, etc., as shown in Figure 12.

In general, a trend surface is mathematically approximated by an n-dimensional polynomial or is obtained using a low-pass filter such as the upward continued filter. Where measuring stations are sparsely located, the shorter wavelength component tends to be also filtered out. Therefore, the Bouguer anomaly distribution of the CG-04 Project (Figure 8), in which the number of measuring stations per unit area is one quarter of the current survey or less, is utilized as the trend surface for estimation of residuals. The result of residual estimation is illustrated in the residual gravity anomaly map.

A profile analysis along the 17 survey lines in the Oued Jebes prospect and the 2 lines in the El Akhouat – Argoub Adama prospect is made so that the gravity residuals match with the subsurface density structures along these measuring lines. The best-fit models for given residuals are interactively approximated for its size and density structure, using the software for magnetic and gravity profile analysis, GM-SYS, developed by Northwest Geophysical Associates Co., Ltd. in USA. Then, the approximated best-fit

models are further refined inversely by computing its size and density structure directly from the residuals. The standard gravity residuals are read on the residual gravity anomaly map. The densities for the subsurface models are expressed in their differences against the correction density for the each prospect.

1. 2. 3 IP survey

The IP survey is carried out for the 17 measuring lines in the Oued Jebes prospect and the 2 lines in the the El Akhouat – Argoub Adama prospect according to the following specifications.

- Electrode Configureuration: Dipole-Dipole Array
- Electrode Spacing (a): 100 m
- Electrode Separation Index (n): 1 to 5
- Transmitted Current: Frequency = 0.125 Hz, Square-Wave with 50 % Duty Cycle
- IP Method: Time Domain
- Equipment Generator: Honda (Japan), Model ET4500 (Max. Output = 4.5 kVA, 3-Phase Alternate, 200 V)
  Transmitter: Phoenix (Canada), Model IPT-3 (Max. Output = 800 V −3.5 kVA)
  Receiver: Scintrex (Canada), Model PR-12(Accuracy = 1 μV)

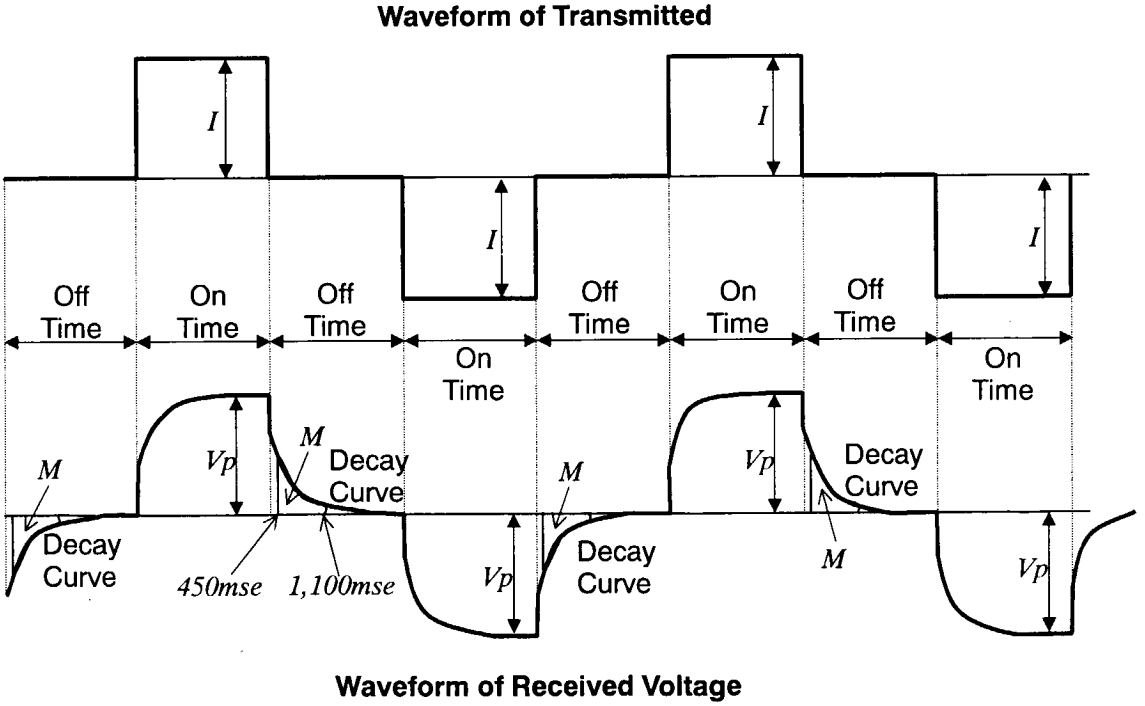

Figure 13 Schematic diagram of time domain IP

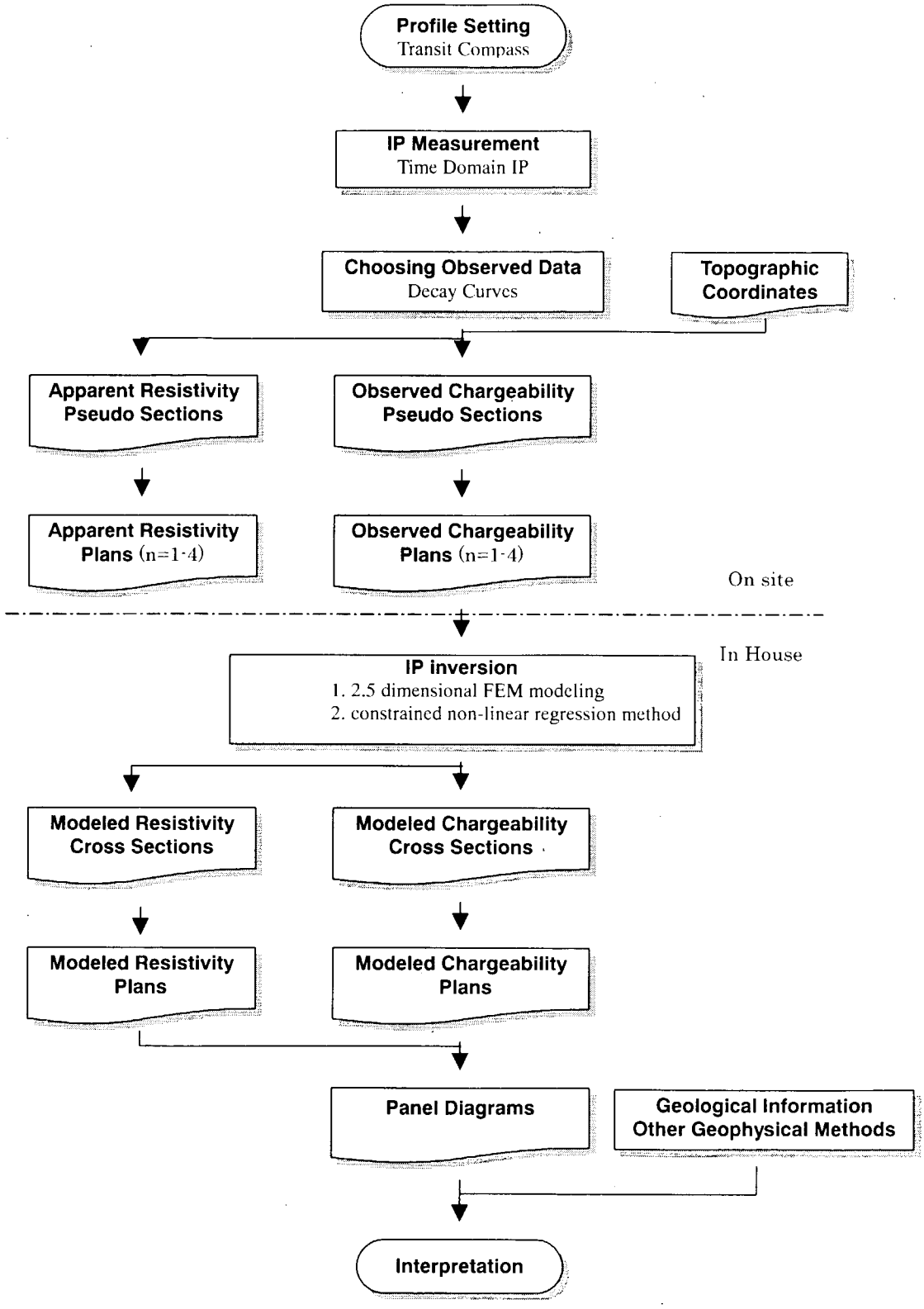

Figure 14 Flow chart of IP Survey

The transmitting dipole, C1-C2, is stationed, while each of the 5 receiving dipoles, P1-P2, P2-P3, P3-P4, P4-P5 and P5-P6 is disposed at a pair of measuring stations in the opposite side. The measurement is made simultaneously at these receiving dipoles. Variation in voltage received at each dipole is shown in Figure 14. Apparent resistivity ρa (Ωm) is estimated, according to the equation (8), for the primary voltage V_p(V) that is the voltage stabilized at a certain level after current I(A) is transmitted.

$$\rho a = K\, Vp / I \tag{8}$$

where K is electrode configuration factor which is estimated for the dipole-dipole array used in the current survey according to the equation (9).

$$K = n(n+1)\,(n+2)\,\pi a \tag{9}$$

a: electrode spacing(m), n: electrode separation index

Chargeability M(mV/V or o/oo) is estimated, according to the equation (10), for the secondary voltage $V_s(t)$(unit: mV) that is a decayed voltage measured at a certain elapsed time after current shut-off. The integration range (t1=450msec–t2=1100msec) for chargeability estimation corresponds to that of the Newmont standard which is normally used in the time domain IP method.

$$M = \frac{1}{Vp\,(t1-t2)}\int_{t1}^{t2} Vs(t)\,dt \tag{10}$$

More than 10 waveforms are collected at one measurement and compared to each other, in order to upgrade S/N (signal/noise) ratio. Although considerable current, averaging 0.3 A, is applied, observed V_p seldom exceeds 1mV due to extremely low ground resistivity. Where V_p is low as is the case, reproducible data can be obtained for apparent resistivity. However, it is very difficult to obtain smooth voltage decay curves. Measurements are repeated two to three times at one measuring station in order to obtain voltage decay curves with acceptable smoothness. Measurements along the survey lines in the NE-SW directions are disturbed by stronger noise than the lines in the NW-SE.

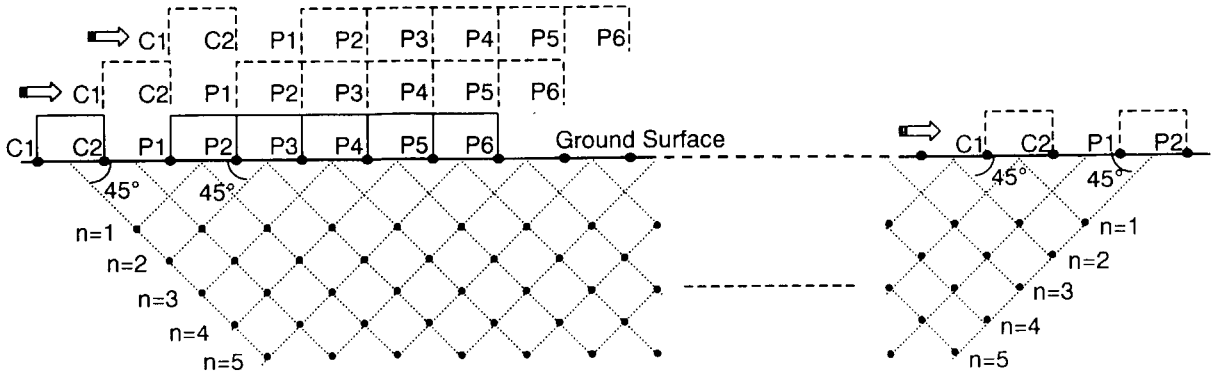

Figure 15 Plotting IP pseudo section with dipole-dipole configuration

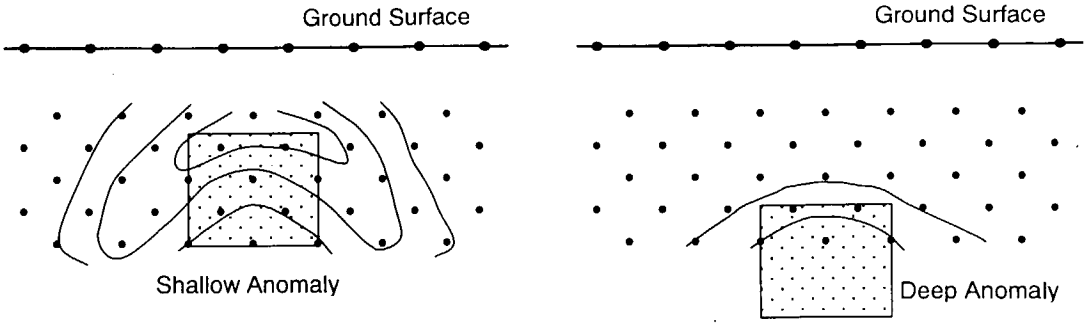

Figure 16 Typical Anomaly Pattern on IP pseudo section with dipole-dipole configuration

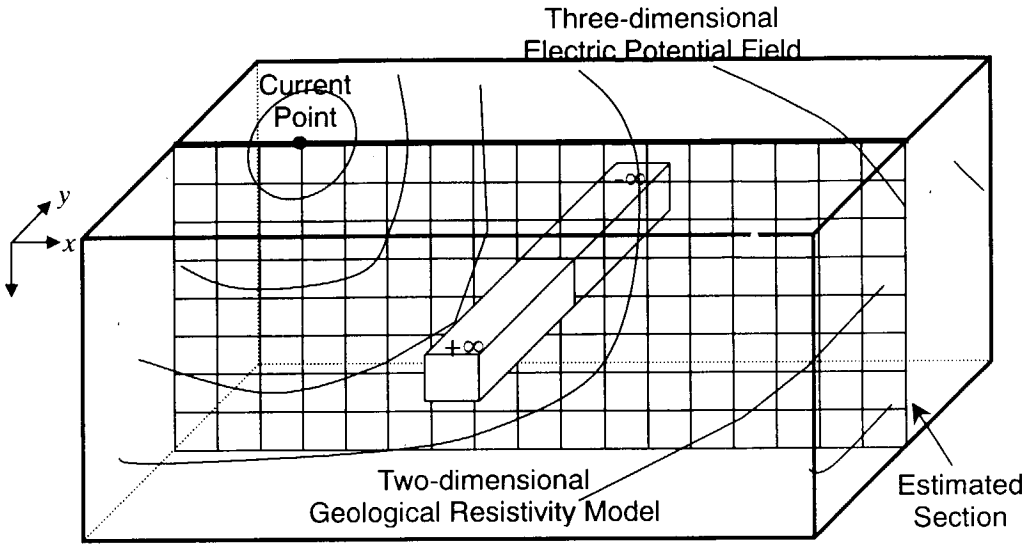

Figure 17 Schematic diagram of 2.5-D resistivity modeling

The measured apparent resistivity and chargeability are presented in pseudo-cross sections of apparent resistivity and chargeability for each survey line according to the plotting procedure illustrated in Figure 15. Based on these pseudo-cross sections, apparent resistivity and chargeability contour maps for the electrode separation indices, n =1,2,3 and 4, are prepared. An anomaly on a pseudo-cross section does not indicate actual geometry of a causative body as shown in Figure 16. It is, therefore, necessary to interpret the anomaly by 2-dimensional modeling analysis for geometry of a causative body on the relevant cross section. In the current investigation, field data are interpreted by combination of the 2.5 dimensional FEM (Finite Element Method) modeling and inversion using the constrained non-linear regression method as proposed by Sasaki (1992). The 2.5 dimensional FEM modeling proposed by Coggon (1977) assumes a prismatic model perpendicular to a cross section extending for a infinitive distance and estimates 3-dimensional voltage distribution applying the Fourier transformation over the assumed prismatic model in accordance with actually transmitted current (Figure 17). This modeling method combined with inversion has been put into practical use by Pelton, et al. (1978).

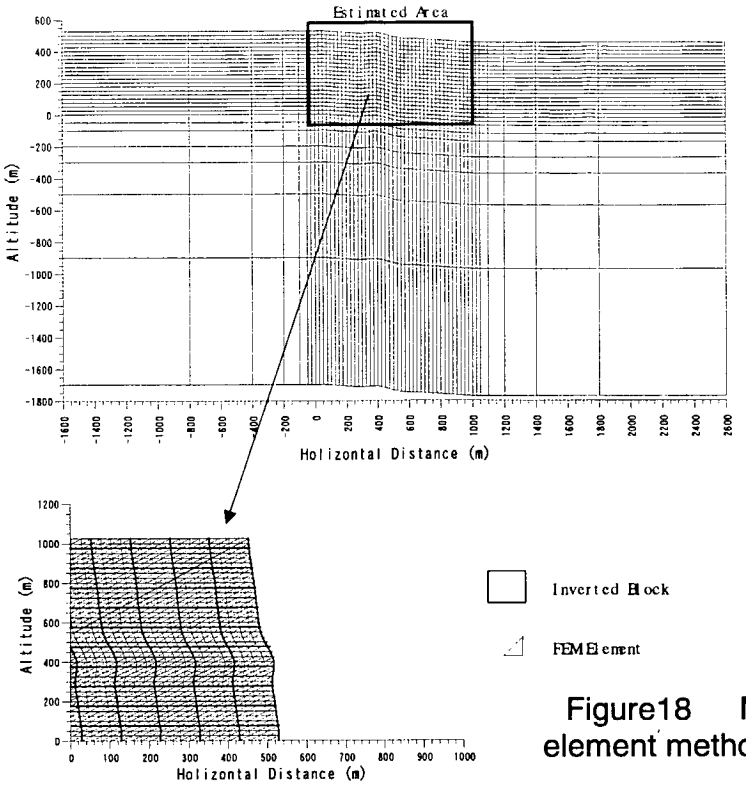

Figure18 Mesh of 2.5-D finite element method and inverted block

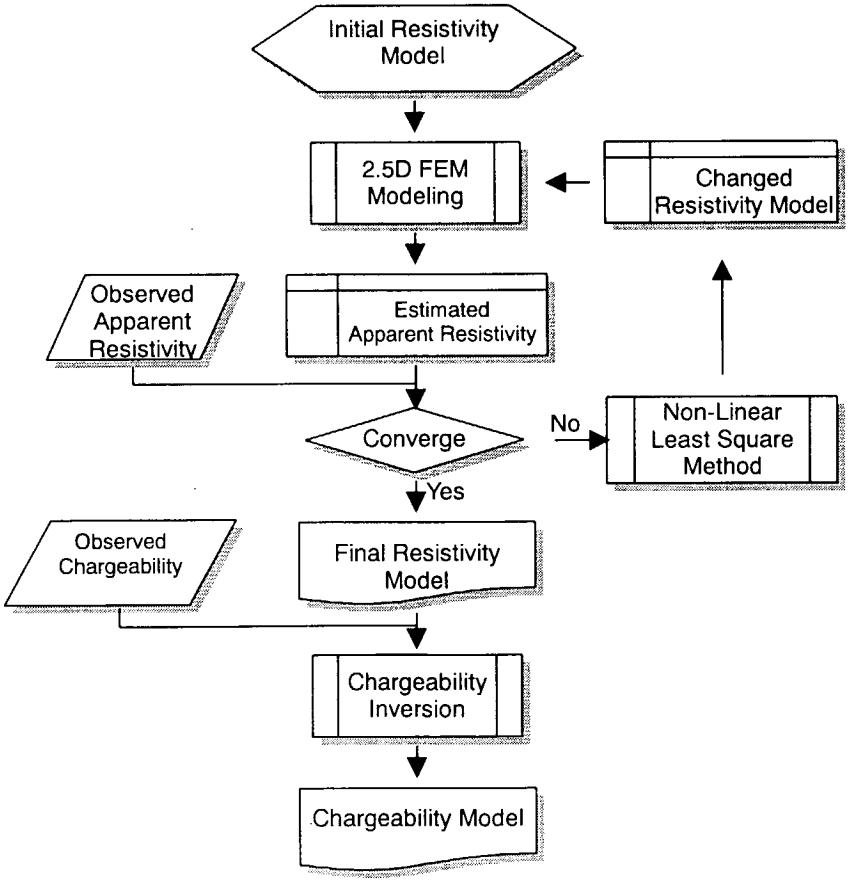

Figure19 Flow chart of IP data inversion

Since inversion of apparent resistivity often becomes ill conditioned, the constraint, called 'Laplacean', is stipulated for its application in order to obtain stable solutions (Dey, et al., 1979). Therefore, the result of inversion is reliable for distribution of apparent resistivity, however, may not necessarily provide absolute values of apparent resistivity or chargeability. Figure 20 indicates elements of FEM used in the cross section analysis and an example of a block interpreted by inversion. A flow of inversion is shown in Figure 21. Interpreted apparent resistivity and chargeability are plotted on cross sections of measuring lines and are illustrated with contours. Contour plans of interpreted apparent resistivity and chargeability for elevations at specified levels above mean sea level are shown.

1.2.4 Laboratory Test

Density, resistivity and chargeability are measured in laboratory for 21 samples collected from outcrops within and around the prospect and shaped into prisms with a width of 4 cm and a length of 8 cm.

Weights of samples are measured in atmosphere and water under 1) natural condition, 2) enforced wet condition, after immersed in tap water for more than 48 hours, and 3) enforced dry condition, after dried in a dry oven for more than 48 hours. Density is estimated using the equations, from (11) through (13). The result is collectively shown in Table 7.

$$\gamma n = W1/(W2-W3) \quad (11)$$

$$\gamma w = W2/(W2-W3) \quad (12)$$

$$\gamma d = W4/(W2-W3) \quad (13)$$

Where,

γn: natural dry density, γw: enforced wet density, γd: enforced dry density

$W1$: weight in atmosphere under natural condition

$W2$: weight in atmosphere under enforced wet condition

$W3$: weight in water under enforced wet condition

$W4$: weight in atmosphere under enforced dry condition

Resistivity ρ and chargeability M are measured using the field equipment of IPR 12 for samples held in GS type sample holders under enforced wet condition. The measurement device is illustrated in Figure 20. The equation (14) is used for estimation of resistivity, while readings of the receiver are converted to chargeability using the equation (10), the same as for the field measurement.

$$\rho = (S/l)(V/I) \quad (14)$$

Where, S: cross section area of sample, l: length of sample

V: received voltage (unit: V), I: transmitted current (unit: A)

Table 7 Results of rock density measurement of specimens

No.	Sample	Geology	Rock	Density (g/cm^3)			Porosity (%)
				γn	γw	γd	
1	A-1	Cretaceous	Limestone	2.39	2.49	2.39	10.50
2	A-2	Cretaceous	Limestone	2.57	2.62	2.57	5.15
3	A-4	Cretaceous	Limestone	2.63	2.65	2.62	2.80
4	A-5	Cretaceous	Limestone	2.55	2.62	2.53	8.52
5	A-6	Cretaceous	Limestone	2.53	2.60	2.53	7.30
6	A-7	Cretaceous	Limestone	2.59	2.62	2.58	3.53
7	A-8	Cretaceous	Limestone	2.65	2.67	2.65	1.41
8	B-2	Cretaceous	Limestone	2.35	2.42	2.35	6.76
9	B-3	Cretaceous	Limestone	2.53	2.61	2.51	10.26
10	B-6	Transition Zone	Celestite ore	3.54	3.57	3.53	3.36
11	B-7	Cretaceous	Limestone with galena vein	2.65	2.68	2.65	3.61
12	B-8	Tertiary	Limestone	2.64	2.64	2.64	0.59
13	B-9	Cretaceous	Limestone	2.56	2.61	2.56	4.98
14	B-11	Tertiary	Sandstone	2.16	2.24	2.06	17.43
15	C-3	Triassic	Calcareous sandstone	2.59	2.62	2.58	4.35
16	C-4	Triassic	Limestone	2.56	2.63	2.55	7.87
17	C-5	Triassic	Dolomite	2.69	2.71	2.69	2.32
18	C-8	Tertiary	Sandstone	2.61	2.70	2.60	10.19
19	C-9	Cretaceous	Mineralized limestone	2.62	2.65	2.61	4.12
20	C-10	Tertiary	Limestone	2.62	2.63	2.62	1.72
21	C-13	Triassic	Dolomite	3.06	3.10	3.04	5.99

Table 8 Results of IP measurement of specimens

No.	Sample	Geology	Rock	Section (cm^2)	Length (cm)	Chargeabilty (mV/V)	Resistivity (Ωm)
1	A-1	Cretaceous	Limestone	16.77	8.09	0.43	420
2	A-2	Cretaceous	Limestone	16.78	8.15	1.45	1,704
3	A-4	Cretaceous	Limestone	19.37	8.26	3.63	5,841
4	A-5	Cretaceous	Limestone	17.21	8.12	4.60	839
5	A-6	Cretaceous	Limestone	18.69	8.03	2.56	1,222
6	A-7	Cretaceous	Limestone	17.01	8.01	5.32	1,455
7	A-8	Cretaceous	Limestone	16.58	8.16	3.36	8,123
8	B-2	Cretaceous	Limestone	16.52	8.11	4.16	387
9	B-3	Cretaceous	Limestone	16.84	8.12	4.82	140
10	B-6	Transition Zone	Celestite ore	16.27	8.10	3.03	1,687
11	B-7	Cretaceous	Limestone with galena vein	18.72	8.22	12.23	2,118
12	B-8	Tertiary	Limestone	16.64	8.19	4.32	14,086
13	B-9	Cretaceous	Limestone	17.75	8.08	1.64	253
14	B-11	Tertiary	Sandstone	17.01	8.01	5.87	58
15	C-3	Triassic	Calcareous sandstone	16.60	8.16	9.62	236
16	C-4	Triassic	Limestone	17.01	8.11	4.38	438
17	C-5	Triassic	Dolomite	16.52	8.16	0.71	6,726
18	C-8	Tertiary	Sandstone	16.89	8.15	7.18	841
19	C-9	Cretaceous	Mineralized limestone	16.94	8.22	12.17	792
20	C-10	Tertiary	Limestone	16.77	8.41	8.19	4,054
21	C-13	Triassic	Dolomite	18.62	8.35	4.61	274

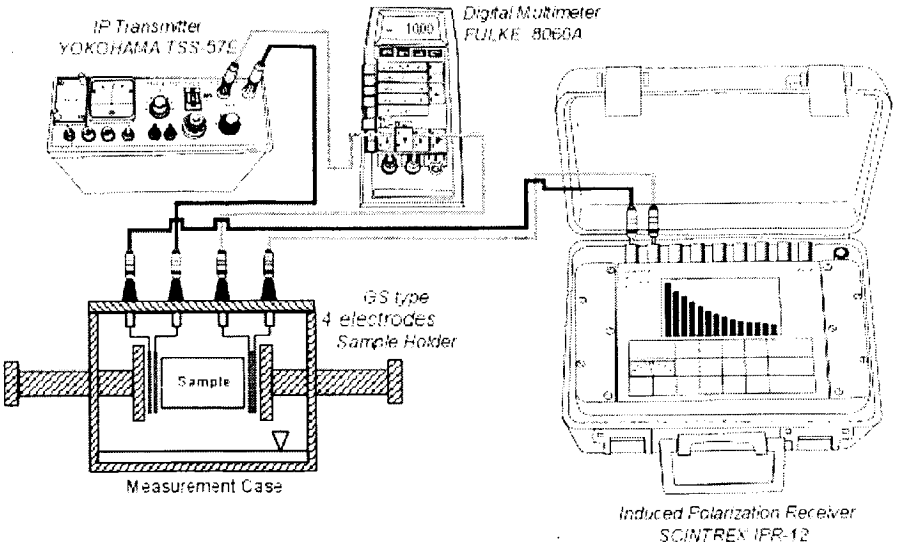

Figure 20 Schematic diagram of IP measurement for a rock sample

The result of resistivity measurement is shown in Table 8. Table 9 shows the result of conductivity measurement of river water, well water and tap water in and around the prospects by using a handy conductivity meter manufactured by the TOA electric wave Co., Ltd. In consideration of the estimated average conductivity of 8,105μS/cm, a NaCl solution of 2,000 μS/cm conductive, equivalent to 5.0 Ωm, was produced for immersing the samples. The solution indicated conductivity of 2,200 μS/cm, at a temperature of 22 degrees Celsius at the time of measurement.

Table 9 Conductivity of water samples acquired in or near the survey area

Sampling Point	Kind of Water	Temperature (℃)	Conductivity (mS/cm)	Resistivity (Ω·m)
Stream near OA prospect	Surface	29.5	9.43	1.060
Stream near OA prospect	Surface	29.5	5.19	1.926
Stream near OA prospect	Surface	29.5	15.15	0.660
Well near OC4	Well	22.0	0.495	20.2
Tap near OA1	Tap	28.2	9.81	1.019
Drill Hole MJTK-A1	Well	26.2	90.5	0.110

1.3 Result

1.3.1 Laboratory Test

Enforced wet densities of 21 rock samples collected in and around the prospects are resulted in the range between 2.24 through 3.57 g/cm^3 from density measurement in laboratory on Table 7. The estimated average density of 2.67 g/cm^3 is higher than the correction density of 2.4 g/cm^3 adopted in the current gravity survey. Around a half of samples are collected from mineral indications sparsely distributed within the prospects. Hard rock samples with better property are measured in the many case of laboratory

test, although many fragile rocks possibly disintegrated during shaping or immersion are lying in the field. The mineralized rocks in the range between 2.65 through 3.57 g/cm^3 and the dolomitic rocks ranging from 2.71 through 3.10 g/cm^3 in the Triassic system show higher density. The density of other rocks, except for 2 rock samples less than 2.50 g/cm^3, ranges between 2.60 and 2.70 g/cm^3.

The results from resistivity and chargeability measurement of 21 rock samples measured density are shown in Table 9. Resistivities ranging from 58 to 14,086 Ωm are averaged around 2,460 Ωm. Rock resistivity ρr is affected by resistivity of pore water ρw and porosity ϕ, as represented following Archie's formula (Archie, 1941).

$$F=\rho r/\rho w=a\phi^{m} \tag{15}$$

Where, F is proportional factor called the formation resistivity factor, a called tortosity factor and m called cementing factor are experimentally estimated in every geological unit. Tortosity factor indicates value around one, cementing factor is ranging between 0.8 and 2.5. The result of the laboratory test appears the average resisitivity of the Tertiary systems higher than that of the older systems. However, it is recommended that the general resistivity of them can't be estimated from only the result of laboratory test because soft rocks are distributed widely the area of the Tertiary systems. The measured resistivities of same kind of geology and rocks vary in one or two orders. The fact suggests that it is very difficult to estimate geological units and rocks according to the resistivity of samples.

The chargeablity of mineralized samples is distigushed clearly from that of the others. The chargeability of the non-minaralized samples is ratively low ranging between 0.4 and 9.6 mV/V, while the 2 mineralized samples indicate high chargeablity more than 10 mV/V except for the celestite sample.

The cross plots on measured density, resistivity and chargeability of samples are shown in Figure 21. Resistive rocks, except for two samples shown higher density than 3.10 g/cm^3, tend to increase density, but their correlation is weak. There is no valid correlation between resistivity and chargeability.

1.3.2 Oued Jebes prospect

(1) Geology

The summary geological plan of the Oued Jebes prospect is shown in Figure 24 respectively. The stratigraphy comprises Triassic systems, Cretaceous system, which consists of Aptian, Alibian, Cenomanian, Turonian and Santonian formation, and Tertiary system, which consists of Eocene, Oligocene, Miocene and Pliocene, overlain by Quaternary system as shown in Figure 24.

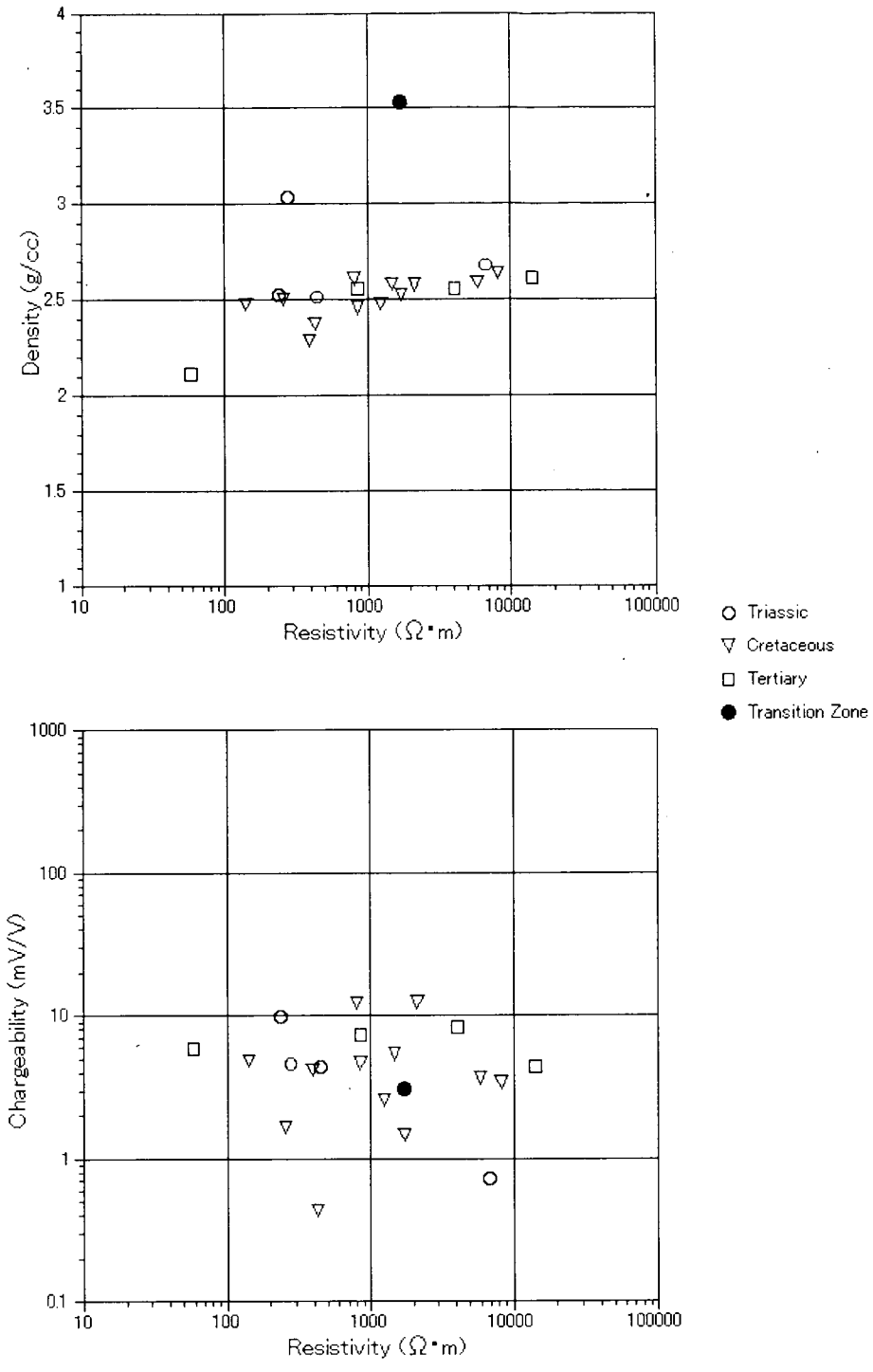

Figure 21 Cross plots of density and chargeability for resistivity of rock specimens

The Triassic systems distribute in the northern, northeastern and southwestern parts of the prospect and form diapers, which is composed of salt rocks in its core and overlying cap rocks such as slate, gypsum, dolomite and so forth.

The Aptian formation comprises mainly alternation of limestone and marl, and distributes in the northeastern part of the prospect. The Albian formation comprises the

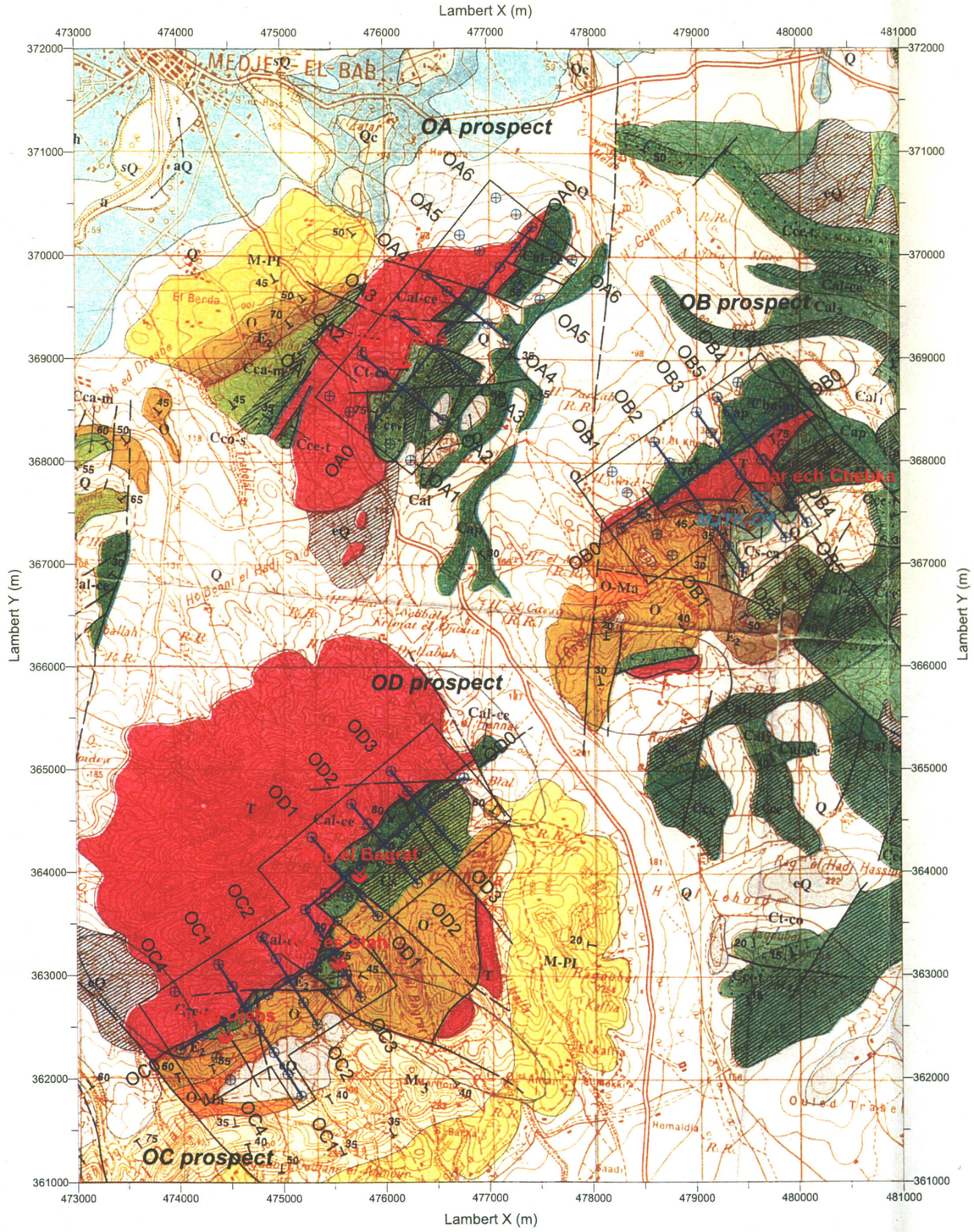

LEGEND

- **a** — *Alluvions récentes des lits d'oueds*
- **sQ** — *a. Silts fins de zone inondable; b. Silts fins de Sebkhas*
- **aQ** — *Argiles et sables de méandres abondonnés*
- **Holocène – Actuel**
- **Qh** — **Holocène** *Argiles sableuses grisâtres à brunâtres*
- **Q** — **Pléistocène supérieur-Holocène** *Argiles sableuses et lits de graviers*
- **cQ** — **Pléistocène moyen à supérieur** *a. Dépôts de pente encroûtés; b. Croûte sableuse feuilletée*
- **Qc** — **Pléistocène moyen** *Sables silteux ocres à concrétions carbonatées et croûte calcaire feuilletée*
- **Pléistocène inférieur** *Argiles sableuses à concrétions carbonatées et croûte calcaire feuilletée*
- **M-Pl** — **Messinien-Pliocène** *Conglomérat, sables et argiles*
- M_3: Miocène supérieur indifférencié
  - M_3^b: *Formation Oued Bel Khédia: Argiles gypseuses, calcaires lacustres et conglomérats*
  - M_3^k: *Formation Kéchabta — a. Argiles et grès à intercalations argileuses; b. Conglomérats rouges*
  - M_3^m: *Formation Oued el Mélah — Argiles gypseuses à intercalations de grès*
- **Mb-l** — **Burdigalien-Langhien** *Argiles et sables*
- **Ma-b** — **Aquitanien-Burdigalien p.p** *Sables et silts rouges*
- **Ma** — **Aquitanien** *Sables,grès,silts et argiles*
- **O-Ma** — **Oligocène supérieur-Aquitanien** *Grès grossiers à dragées de quartz*
- **O** — **Oligocène** *Calcaires gréseux bioclastiques, argiles vertes et grès*
- **E_2** — **Eocène supérieur** *Argiles avec rares intercalations carbonatées à la base*
- **E_1** — **Eocène inférieur** *Calcaires massifs à Globigérines et/ ou à Nummulites*
- **Cm-p** — **Paléocène** *Argiles*
- **Cca-m** — **Campanien-Maastrichtien** *Marnes et calcaires*
- **Cs-ca** — **Santonien-Campanien** *Marnes et calcaires*
- **Cs** — **Santonien** *Murnes et calcaires*
- **Cce-t** — **Coniacien-Santonien** *Marnes et calcaires*
- **Cco** — **Coniacien** *Marnes et calcaires*
- **Ct-ce** — **Turonien supérieur-Coniacien** *Marnes et calcaires*
- **Ct** — **Turonien** *Calcaires et marnes*
- **Cce-t** — **Cénomanien supérieur-Turonien inférieur à moyen** *Calcaires gris à jaunâtres*
- **Cm** — **Cénomanien inférieur à moyen** *Alternances de marnes grises et de calcaires en plaquettes*
- **Cal-ce** — **Albien supérieur-Cénomanien basal** *Calcaires feuilletés en plaquettes, à Ammonites*
- **cQM** — **Albien indifférencié**
- **Cal** — **Albien moyen et supérieur** *Marnes et calcaires en plaquettes*
- **Cs** — **Albien inférieur** *Calcaires massifs noirs*
- **Cap** — **Aptien** *Alternances de calcaires et de marnes feuilletées*
- **Cbs-ap** — **Barrémien-Aptien** *Argiles gréseuses, calcaires et marnes*
- **Cb-hr** — **Hautérivien-Barrémien inférieur** *Calcaires, marnes et argiles gréseuses*
- **Cv** — **Valanginien** *Argiles silteuses, grès, calcaires et marnes*
- **Jd** — **Dogger** *Calcaires noduleux, pélites et calciturbidites*
- **Jl** — **Lias** *Dolomies et calcaires*
- **T** — **Trias** *Argiles, dolomies et gypses*

Limite stratigraphique

Faille — a. Vue; b. Supposée

Pendage — a. Normal; b. Horizontal; c. Inverse

Loupe de glissement

Survey Prospect

Profiles for IP survey

Gravity Station

Ancient Works

Diamond Drill-Hole

0 1000 2000 3000 4000 5000 (m)

Figure 22 Geological map of Oued Jebs prospect

limestone and the marl members, and distributes from the northeastern to the southeastern part of the prospect. The Cenomanian formationdistributes from the northeastern to southern part of the prospect and comprises alternation of limestone and marl. The Turonian formation distributes in the northeastern to southwestern part of the prospect and in the vicinity of the Triassic diapers, and consists of limestone and marl. The Santonian formation distributes in the eastern and the northwestern part, and comprises limestone and argillaceous limestone members.

The Eocene distributes in the northwestern, eastern and southeastern parts of the prospect and consists mainly of marl and argillaceous limestone. The Oligocene distributes in the central, southern and northwestern parts, and comprises alternation of sandstone and argillite with the limestone. The Oligocene-lower Miocene distributes in the central part, and mainly consists of coarse-grained sandstone. The Miocene distributes in the southern part, and mainly composed of argillite. The Miocene-Pliocene distributes in the northwestern and southern parts of the prospect, and consists of conglomerate, sand and clay.

The Quaternary System comprises talus deposits, colluviums and alluviums. The terrace deposits and colluviums distribute over hilly terrain or around foothills, comprising gravel, sand and clay, while alluviums, also consisting of gravel, sand and clay, develop along rivers and major streams or over low lands in their vicinity.

The geological structure of the general area, hence of this prospect, is characterized by extensive development of diapirs and faults. NW-SE trending faults are developed. The NE-SW and E-W trending faults are crosscutting the NW-SE trending faults.

(2) Gravity survey

Characteristics of Bouguer anomaly (hereinafter called 'gravity') distribution in the OA, OB, OC and OD sub-prospects are described below.

①Regional Gravity Distribution (Figures 8)

In the gravity map of the Mejez el Bab quadrangle including OA, OB, OC and OD sub-prospects, the great area of gravity high exceeding 13 mgal centering in the vicinity of the Lambert coordination of 47,490E and 36,700N in the central part of the quadrangle is remarkable. Three high gravity anomalies beyond 18 mgal lie within the gravity high. The great area of the gravity high stretches in the NW-SE direction. The steep gravity gradient in the eastern margin of it extends in the N-S direction, the northern and southern margins become the steep gravity gradients stretching in the E-W direction. The N-S and the E-W gravity trends are predominated in the east sides of the gravity high. In the opposite side, the NE-SW and crosscutting NW-SW gravity trends are predominated parallel to the regional geological structures in the Krib-Mejez el Bab project area.

The four sub-prospects in the Oued Jebes prospect investigated in the current program are located inside and in the marginal area of the extensive gravity high in the central part of the quadranle. The Bou K'hil, the El Akhouat, the Bazina Kebira and the Siliana prospects investigated in the previous program and the Fejera Doume working mine are located in and around gravity high. Though diapirs tend to be related to gravity high, a diapir is generated by rise of a low-density rock mass upwards. The fact suggests that rising geological structures upwards such as anticline increase gravity and diapers go up along the fractures generated above the structures.

②Gravity Distribution of the Prospect (Figure 23)

The OA sub-prospect lies in the west marginal area of the extensive gravity high in the central part of the regional gravity map. The low gravity cut from the great gravity low of the west side into the gravity high in the vicinity of the sub-prospect. The low gravity runs from the north to the south around the Bou Mouss old working.

The OB sub-prospect lies in the southwest margin of the high gravity anomaly exceeding 18 mgal in the north side of the center of the extensive gravity high. The low gravity runs from the south to the north in the vicinity of the Dar ech Chebka small old working.

The OC sub-prospect lies in the southwest marginal part of the extensive gravity high. The gravity high juts up around the Oued Jebes old working. The Kef Lasfer small old working is located in the jutted part of the narrow gravity high stretching from the northwest to the southeast along the survey line OC3. This narrow gravity high seems to the part lying between two small low gravity anomalies.

The OD sub-prospect lies around the small high gravity anomaly beyond 18 mgal in the southwestern part of the extensive gravity high. The low gravity anomaly cut into the small high gravity anomaly of the north side in the vicinity of the Rag el Bagrat mineral indication.

These features suggest that the mineral occurrences in the Oued Jebes prospect are located around the low gravity anomalies within the extensive gravity high.

③Residual Gravity Anomaly (Figure 24)

The residual gravity distribution in the OA sub-prospect is characterized the low anomaly below –0.2 mgal running from the southwest to northeast in the northwestern side of the base line OA0. The fact that this low residual gravity anomaly corresponds to the area of the Triassic system suggests that a low-density diapir shows the anomaly.

The residual gravity distribution in the OB sub-prospect is characterized the low anomaly running from the southeast to the northwest along the survey line OB0. Within this the low residual anomaly the tertiary systems distribute wider than the Triassic systems. However, it is possibly guessed that the low residual gravity anomaly is generated by geological structures such as fractures related to rise of Triassic diapir